The Pennsylvania State University

The Graduate School

Department of Electrical Engineering

FABRICATION OF LONG PERIOD GRATINGS FOR ULTRA-FAST TUNABLE FILTER

A Thesis in

Electrical Engineering

by

Corey Allan Hahn

Submitted in Partial Fulfillment
of the Requirements
for the Degree of

Master of Science

May 2005

Corey Allan Hahn

The thesis of Corey Allan Hahn was reviewed and approved* by the following:

Shizhuo Yin
Associate Professor of Electrical Engineering
Thesis Advisor

Karl Reichard
Assistant Professor of Acoustics
Thesis Co-Advisor

Zhiwen Liu
Assistant Professor of Electrical Engineering

W. Kenneth Jenkins
Professor of Electrical Engineering
Head of the Department of Department of Electrical Engineering

*Signatures are on file in the Graduate School

ABSTRACT

Development of better optical filtering devices is of paramount importance to applications that demand harsh environment conditions and better performance characteristics. Lower insertion loss, tuning range, tuning speed, and bandwidth are just some important qualities in a superior fiber optic filter. An all fiber, tunable filter based on a single resonant band long period grating has many of these important qualities. Fabrication of a novel filter design based on a three layered approach to the optical waveguide in a fiber involves many steps each with their own problems and hurdles. Producing the filters encompassed many different facets of etching, grating writing, sputtering, polymer application, and testing. In this thesis, various methods for producing a three layer, ultra-fast tunable filter based on a long period grating are examined.

TABLE OF CONTENTS

LIST OF FIGURES

ACKNOWLEDGEMENTS

I want to convey my love and appreciation to my wife Mary for her constant support and encouragement. I would also like to express my gratitude to my parents and family for their support and assistance. Also, I thank Professors Karl Reichard, Zhiwen Liu, and my advisor Shizhuo Yin for their academic guidance. Finally, I am very grateful to the members of the electro-optics lab, in particular, Jon Lee and Sung Hyun Nam for all their help and encouragement. This material is based upon work supported by the Penn State Electro-Optic Center, sponsored by the Naval Air Systems Command under Contract Number N00421-03-D-0044, Delivery Order Number 01.

Chapter 1

Introduction

1.1. Motivation

Filtering light is a fundamental process in communication devices. Filters in the RF region of the Electromagnetic spectrum were a basic building block for early communication devices. Through the years as the carrier frequency has moved farther and farther higher, new techniques for producing reliable filters had to be developed so that the communication at that carrier could be reliable. Today the carrier has progressed into the near infra-red and visible regions of the spectrum. Modulated light traveling down fiber optic cables or waveguides needs filters to demodulate, direct, and shape the light.

As fiber optic technology evolves toward a newer generation of speed and flexibility the devices associated with the fiber technology also has to advance to support the ever increasing demands on bandwidth and data speed. Fiber technology has progressed to the point where the fiber is making its way into harsh environments and applications that traditionally only electronic communication lines and sensors existed. Bandwidth requirements, interference, and interface issues are forcing fiber to take these new roles and forcing the community to find the answers to make the fiber work. Current technology could not fill the voids in speed, response time, and reliability. Our goal is to produce a filter for these applications and improve the performance and reliability of

these devices. More specifically it was our goal to produce a filter with low insertion loss less than 0.5 dB, wide tuning greater than 50 nm, and a 3dB bandwidth that could be from 0.1 – 20 nm. These goals would put the device in the forefront of many tunable filter applications.

1.2. Background

Long period gratings are the tuning mechanism in the filter design. Lopez-Higuera defines gratings as "An optical fiber with a periodic refractive index perturbation pattern inscribed in the core such that it diffracts the optical signal in the guided mode at specific wavelengths into other core-bounded modes, cladding modes, or radiation modes [1]." Long period gratings (LPG) can couple the modes between the fundamental core mode and the cladding modes traveling in the same direction [3]. Since this coupling is wavelength selective, both fixed and the tunable wavelength filters based on this effect have been developed [3-8]. One of the unique features of an LPG is that it is highly sensitive to the cladding refractive index. To achieve a wider tuning range and better quality spectrum we have developed a unique single resonant band LPG by using an ultra-thin cladding layer [9-14]. A quantitative analysis of the performance of the filter was performed based on a three-layer model [15-16], and from this model we developed filter designs that serve as an effective method to tune the resonant wavelength by using a second electro-optic cladding layer. As the refractive index of the second layer is modified by an applied voltage the resonant wavelength filtered by the LPG device is changed.

Current technologies to tune and filter light traveling in a fiber optic are largely limited by their speed, tuning range, or cost. One such example is fiber Bragg gratings that are stretched or thermally tuned. Using Bragg gratings offers advantages such as very narrow 3 dB bandwidths (.2 nm) and low insertion loss (.1 dB). The tuning mechanism lends itself to slow tuning rates and failure due to the mechanical nature of physically heating or stretching the fiber. Another approach is to use a cascade of Mach-Zender interferometers. Since MZIs operate due to an EO effect, the tuning speed is quite fast (50 ns), but the insertion loss in such a device is not acceptable for most applications (19 dB). Using an all fiber approach gets by the insertion loss hurdle. Fiber Bragg gratings utilize this, although it is imperative for most applications that the tuning range be widened and that the actual tuning mechanism not be a mechanical process. Utilizing an electro-optic effect for the switching mechanism we can utilize a high speed tuning mechanism as well as shed the need for mechanical tuning. Finding a way to create an electro-optic and all fiber device is the answer.

Chapter 2

Theory

2.1. Coupled Mode Theory and Filter Operation

In a standard single mode fiber with an LPG in the core, coupling between the core mode and cladding modes varies with wavelength. Since the cladding supports many modes, the difference between the effective indices of the cladding modes is small for a given wavelength. The small difference between the effective indices of the cladding modes gives rise to resonant peaks at several signal wavelengths in the spectral response of a fixed period LPG. Multiple resonant peaks are detrimental to LPGs use in tunable filter applications because they limit potential tuning range and performance.

In order to obtain a single resonant band in the spectral response, an ultra thin cladding layer is used. The thinner cladding limits the number of modes that will propagate, and the difference between the effective indices of each cladding mode is significantly increased. With this increase, a single resonant band over the entire near infrared spectrum (i.e. 1000 nm to 1700 nm) can be achieved, and the LPG is no longer limited by the potential tuning range.

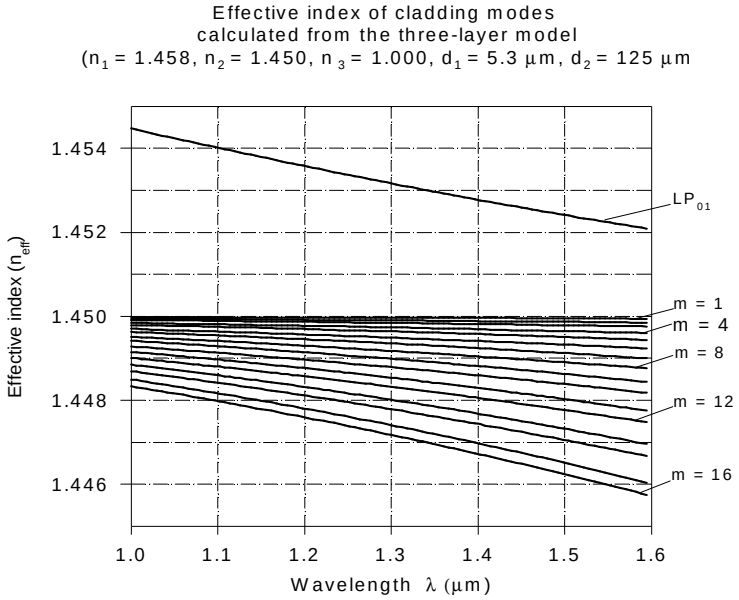

Figure 1. Effective refractive indices for the core and cladding modes in a standard single mode fiber.[18]

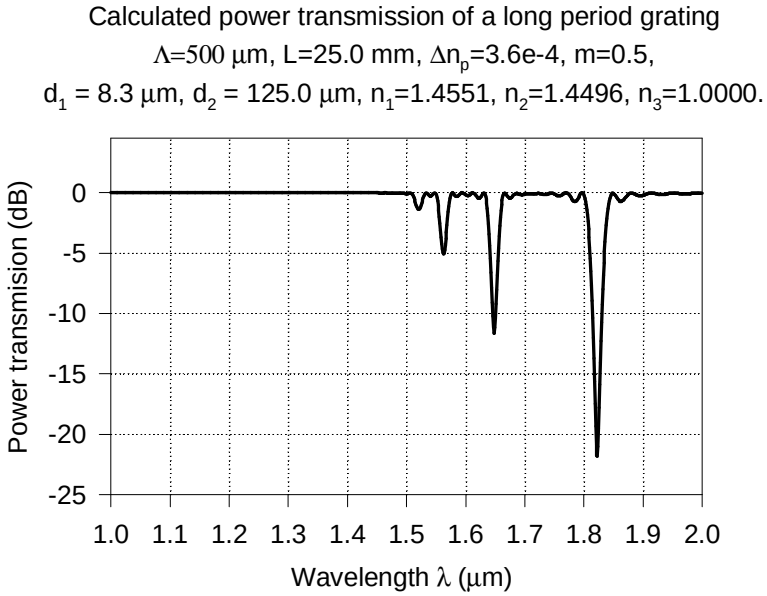

Figure 2. Spectral response of an LPG in a standard single mode fiber.[18]

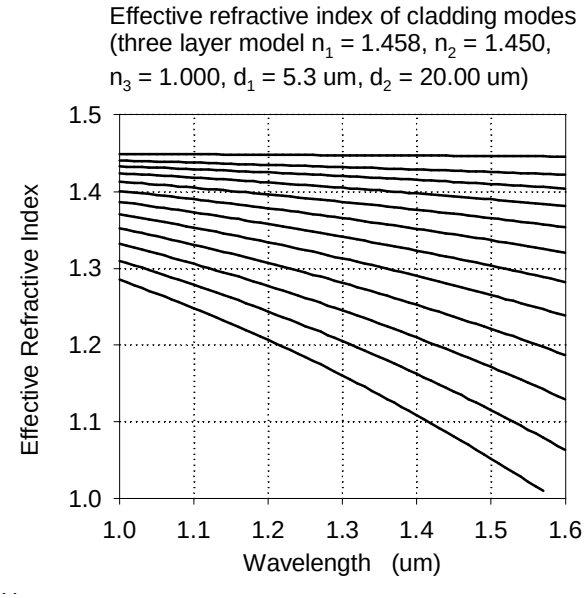

Figure 3. Effective refractive index of cladding modes in single mode fiber with ultra thin cladding.[18]

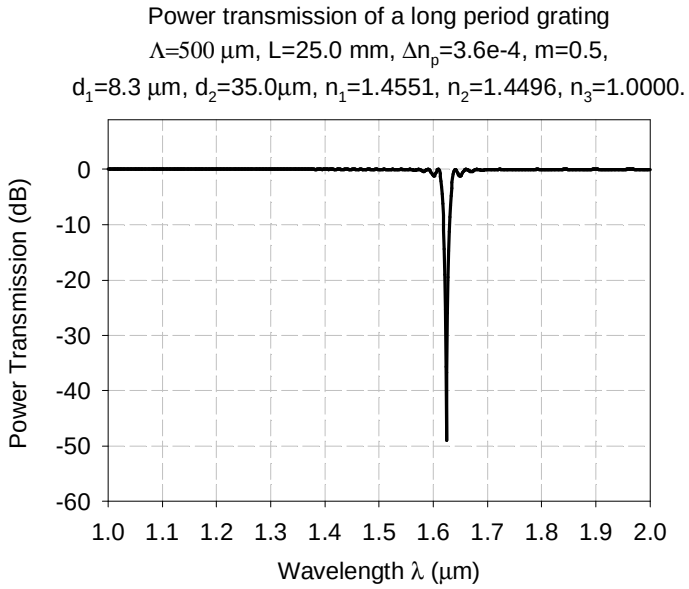

Figure 4. Spectral response of single mode fiber with ultra thin cladding.[18]

The effective index of the cladding-modes is very sensitive to the surrounding medium, and the wavelength response of the LPG filter can be tuned by varying the index of the surrounding material. A second cladding layer made of electro-optic polymer is used to tune the device.

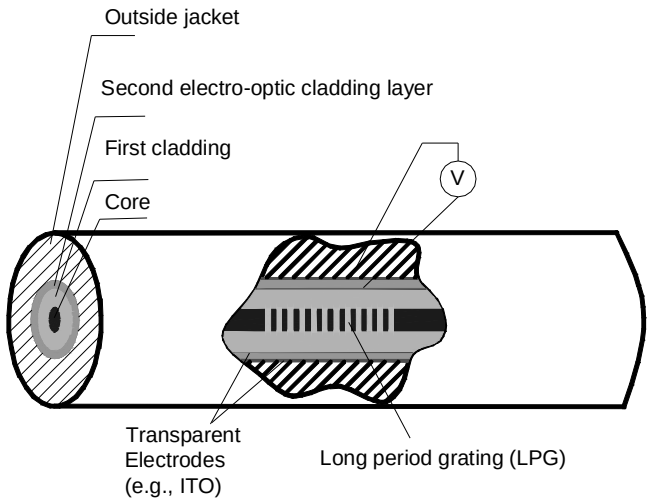

Figure 5. Tunable optical filer based on LPG and double cladding structure.

By applying an external electric field, the index of reflection of the second cladding layer can be changed. As a result, the effective index of the first cladding layer changes, and the filtered wavelength, $\lambda = (n_{eff\_co} - n_{eff\_cl})\Lambda$, can be selected by controlling the external electric field.

The performance characteristics of this filter give it an advantage over other filtering technologies currently available. The LPG filter boasts high sensitivity, a wide tuning

range, fast tuning speed, and a narrow bandwidth. The sensitivity of the device can be demonstrated by taking the derivative of the equation for LPG coupling.

$$\lambda = (n_{eff\_co} - n_{eff\_cl})\Lambda$$

The relationship between the resonant wavelength shift and the refractive index modulation can be written as,

$$\Delta\lambda = \frac{\Delta(n_{eff\_co} - n_{eff\_cl})}{n_{eff\_co} - n_{eff\_cl}} \approx \frac{\Delta n_{eff\_cl}}{n_{eff\_co} - n_{eff\_cl}}$$

Since n_{eff_co} and n_{eff_cl} can be very close with a thin cladding, a small change in Δn_{eff_cl} induces a large change in the resonant wavelength, and the LPG can be tuned easily by adjusting the index of the second cladding.

The spectral bandwidth of the LPG is proportional to λ/N, where λ is the resonant wavelength and N is the total number of grating periods. Using this relationship, a large number of grating periods are required to achieve a narrow bandwidth (e.g. < 1 nm). For example, the maximum difference between the effective indices of the core and the lowest 15 cladding modes (i.e. n_{eff_co} - n_{eff_cl}) is 0.01 in a conventional LPG. For the resonant peak to fall in the near infrared range (i.e. λ= 1.0 µm), the grating period would be greater than 100 µm. For a narrow bandwidth filter, the grating length would have to

be on the order of 300-500 mm, which is unacceptably long. The ultra thin cladding provides for a narrow 3 dB bandwidth by increasing the difference between the effective indices of the core and cladding modes. If the difference between the indices is increased to 0.1, the resonant wavelength can be in the 1.55 μm range, and the grating period can be shortened. This, in turn, shortens the length needed for a large number of grating periods and subsequently, a narrow bandwidth.

The effective index of the core (n_{co_eff}) is a function of the material indices of the fiber core and the ultra-thin cladding region, n_1 and n_2, respectively, which is determined by the following dispersion relationship,

$$V\sqrt{1-b}\,\frac{J_1(V\sqrt{1-b})}{J_0(V\sqrt{1-b})} = V\sqrt{b}\,\frac{K_1(V\sqrt{b})}{K_0(V\sqrt{b})}$$

Where J_m (m = 0, 1) is a Bessel function of the first kind, K_m (m = 0, 1) is a modified Bessel function of the second kind, and b is the normalized propagation constant defined as:

$$b = \frac{(\beta / k_0) - n_2}{n_1 - n_2} = \frac{n_{eff\_co} - n_2}{n_1 - n_2}$$

The cladding's effective index (n_{eff_cl}) is a function of n1, n2, and n3, where n3 is the refractive index of the electro-optic polymer. Solving the dispersion relation equation will produce a n_{eff_cl} [18].

$$\zeta_0 = \zeta_0'$$

where

$$\zeta_0 = \frac{1}{\sigma_2}\frac{u_2(JK + \frac{\sigma_1\sigma_2 u_{21}u_{32}}{n_2^2 a_1 a_2})p_l(a_2) - Kq_l(a_2) + Jr_l(a_2) - \frac{1}{u_2}s_l(a_2)}{-u2(\frac{u_{32}}{n_2^2 a_2}J - \frac{u_{21}}{n_1^2 a_1}K)p_l(a_2) + \frac{u_{32}}{n_1^2 a_2}q_l(a_2) + \frac{u_{21}}{n_1^2 a_1}r_l(a_2)},$$

$$\zeta_0' = \sigma_1 \frac{u_2(\frac{u_{32}}{a_2}J - \frac{n_3^2 u_{21}}{n_1^2 a_1}K)p_l(a_2) + \frac{u_{32}}{a_2}q_l(a_2) + \frac{u_{21}}{a_1}r_l(a_2)}{u_2(\frac{n_3^2}{n_2^2}JK + \frac{\sigma_1\sigma_2 u_{21}u_{32}}{n_1^2 a_1 a_2})p_l(a_2) - \frac{n_3^2}{n_1^2}Kq_l(a_2) - \frac{n_3^2}{n_1^2}Kq_l(a_2) + Jr_l(a_2) - \frac{n_2^2}{n_1^2 u_2}s_l(a_2)}.$$

The following definitions have been used in the dispersion relation equation above:

$$\sigma_1 \equiv i\ln_{ef}\ f / Z_0$$
$$\sigma_2 \equiv i\ln_{eff}\ Z_0$$
$$u_{21} \equiv \frac{1}{u_2^2} - \frac{1}{u_1^2}$$
$$u_{32} \equiv \frac{1}{w_3^2} + \frac{1}{u_2^2}$$

where

$$u_j^2 \equiv (2\pi/\lambda)^2 (n_j^2 - n_{eff}^2), [j \in (1,2)],$$
$$w_3^2 \equiv (2\pi/\lambda)^2 (n_{eff}^2 - n_3^2),$$
$$J \equiv \frac{J_l'(u_1 a_1)}{u_1 J_l(u_1 a_1)},$$
$$K \equiv \frac{K_l'(w_3 a_2)}{w_3 K_l(w_3 a_2)},$$
$$p_l(r) \equiv J_l(u_2 r) N_l(u_2 a_1) - J_l(u_2 a_1) N_l(u_2 r),$$
$$q_l(r) \equiv J_l(u_2 r) N_l'(u_2 a_1) - J_l'(u_2 a_1) N_l(u_2 r),$$
$$r_l(r) \equiv J_l'(u_2 r) N_l(u_2 a_1) - J_l(u_2 a_1) N_l'(u_2 r),$$
$$s_l(r) \equiv J_l'(u_2 r) N_l'(u_2 a_1) - J_l'(u_2 a_1) N_l'(u_2 r).$$

Creating defects in the material is one way for changing the index of refraction. Defect creation modifies the absorption of the material and through the Kramers-Kronig relationship the index is also affected. The dispersion relationship between absorption and refractive index allow this modification of the fiber in defined areas to contribute to the grating pattern.

2.2. Hydrogen Loading and Ultraviolet Induced Defect Creation

Loading fiber strands with Hydrogen increases their susceptibility to the ultra-violet light induced index perturbations. Commercial fiber (silica) when manufactured has many inherent defects. The processes used in making fiber glass such as modified chemical vapor deposition creates soot that is deposited on the inside of a silica support tube, and then is annealed. During this process the germanium used as a dopant in the silica is deposited alongside the silica. The final drawn fiber has many defects from the strained non-crystalline structure, dopant, and the drawing process itself. Germanium is often the dopant in commercial fiber and during the manufacturing process forms oxides in the

silica structure. Germanium oxides embedded in the silicon dioxide lattice can become electronically active upon UV illumination. The active Germanium atoms then become the source of absorption in the silicon. The concentration of the Germanium defects controls the amount of change in the dispersion in the fiber and thus index. [1]

Germanium doping does not work for every application due to cost and sensitivity of germanium defects to UV light. Hydrogen loading is another process by which either normal commercial fiber or Germanium doped fiber is subjected to high pressure and/or high temperature hydrogen causing the hydrogen atoms to migrate into the fiber. UV light is used as a catalyst for reducing the Germanium from GeO to GeH. Changing the molecular makeup of the material affects the absorption, causing an index change on the order of .01. Without Hydrogen loading, UV induced index change is only on the order of .001. The drawback of this method is the losses incurred by the production of OH- ions, which can cause significant absorption in the communications bands. Heavier Deuterium is often used to get by this problem by shifting this absorption further into the infrared (~1900 nm). After loading, the fibers have to be written quickly because the Hydrogen will begin to diffuse from the fiber once high pressure and temperature conditions are relaxed. [1]

2.3. Indium Tin Oxide Sputtering

Sputtering is the use of a low pressure inert gas which is usually argon to physically bombard a target, release target atoms, and then deposit these atoms on a substrate. In DC sputtering a voltage is placed across a gap with the cathode holding the target and the

substrate attached to the anode. The argon ions present in the cavity between the two are then ionized and separated into Ar^+ ions and electrons. The positive argon atoms then accelerate toward the negative cathode and strike the target's surface, dislodging atoms. The target atoms are then free to travel in the chamber and deposit on the substrate.

The sheath or dark space between the cathode plasma and the argon plasma is the driver of the process. As argon atoms are ionized by electrons passing from the cathode to the anode, they migrate towards the sheath and then are accelerated by the voltage drop in this area. The increased velocity then aids the argon's ability to sputter target ions. Secondary electrons are produced from the bombardment and accelerated towards the argon plasma and the process sustains itself.

Normal direct current sputtering is not suitable for insulator deposition like indium tin oxide (ITO). The biggest problem is applying the necessary voltage to the target to ignite the plasma. Radio frequency sputtering is used instead to capacitively couple through an insulating target. The frequency 13.56 MHz is set aside specifically for RF sputtering. This frequency is high enough that the electrons' mobility allows them to keep up with the changing electric field, but the argon ions are too massive to react.

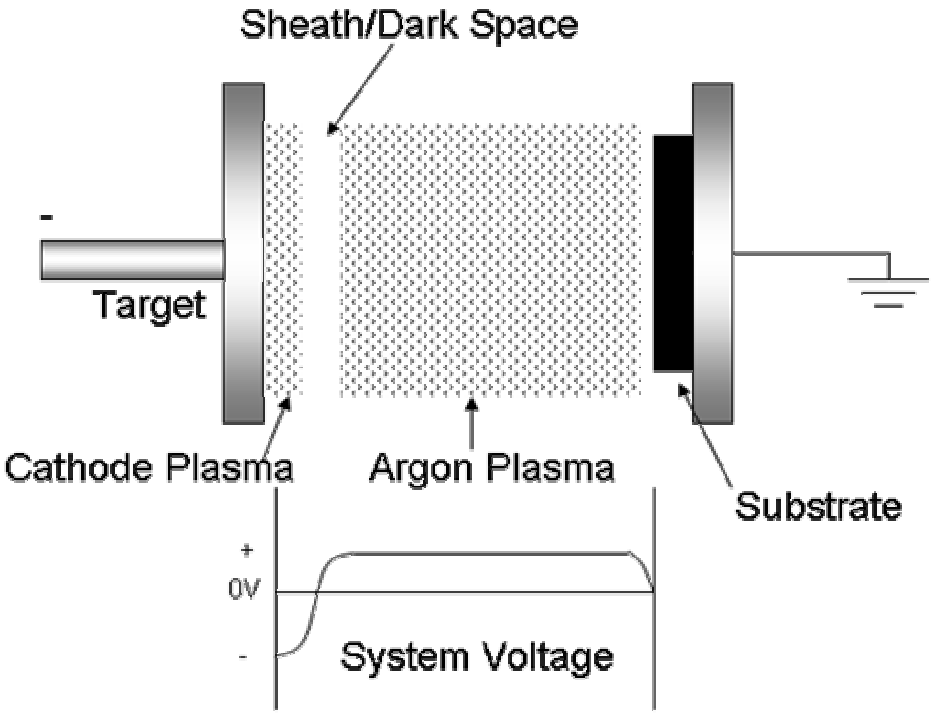

Figure 6. DC sputtering plasma structure and voltage distribution.

Magnetron sputtering increases the efficiency and speed of the RF sputtering. Using magnets placed behind the target, the electrons are confined to the space directly above the cathode thus increasing the likelihood that an electron-argon collision will occur. The magnetic field oriented perpendicular to the electric field causes the electrons to spin in a spiral near the target's surface. If the rate of creation of argon ions can be increased sputtering speed will also increase. It is this effect that causes the characteristic donut shaped plasma that forms on the surface of the target [17].

Indium Tin Oxide (ITO) is a material that is commonly used in industry to form a clear conductive surface. Composed of 90% Indium oxide and 10% Tin oxide, these films are

transparent (>80%) to the visible spectrum and can reach sheet resistances of less than 10 Ω/sq. [20]

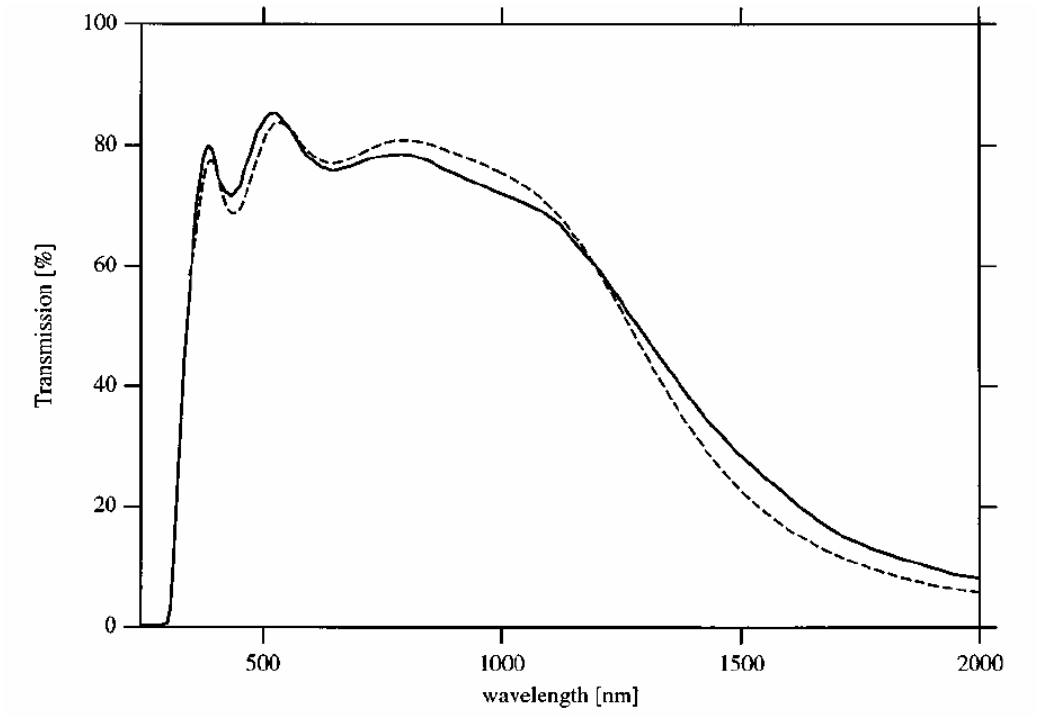

Figure 7. ITO transmission spectra. Theoretical (dotted) and measured with ellipsometry. [19]

ITO has good transparency in the UV region which allows the writing of gratings after a thin film has been deposited. Caution has to be taken in that the ITO's sheet resistance can be lowered with thicker deposition, but with its index 1.95 in the visible and reflective in the infrared (>80%), application has to be a balance between conductivity and transmission of filtered wavelengths. [20]

Chapter 3

Method of Procedure

3.1. Overview of Process

Currently the processes involved in producing a device from fiber and polymer is involved and at best takes several days. The current method entails taking fiber, etching it down to an ultra-thin cladding, sputtering a conductive transparent layer, writing a grating, applying a polymer, sputtering an outer conductive layer, and packaging the device. At each stage the progress of the device is checked for accuracy and deviation from the normal parameters that have been recorded from earlier devices.

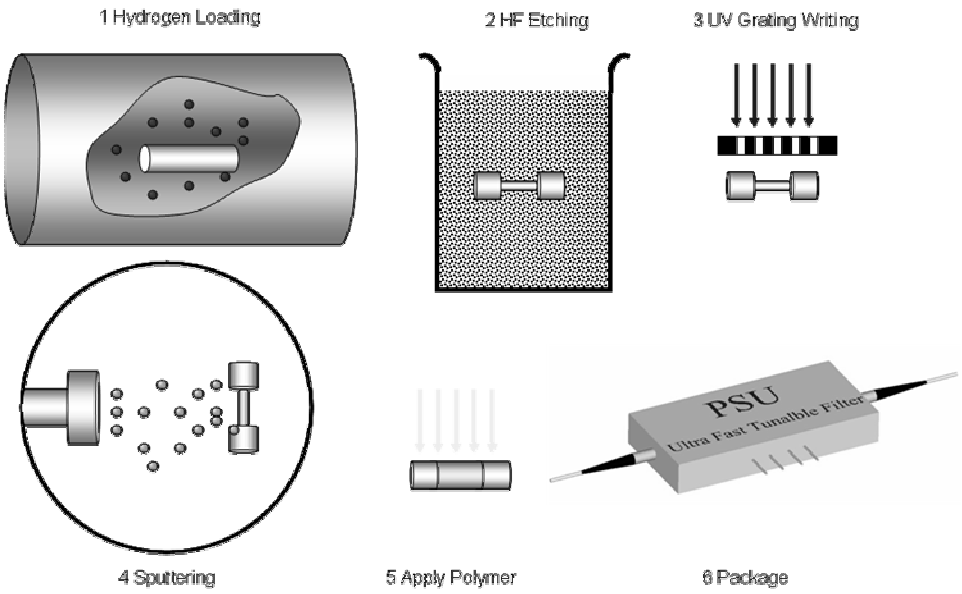

Figure 8. Process overview of filter construction.

3.2. Preparation and Hydrogen Loading

Construction of the device begins with either photosensitive fiber (F-SBG-15) obtained from the Newport Corporation or hydrogen loaded commercial fiber from Corning (SMF-28e). Loading the fiber with hydrogen starts with stripping of the fiber at 450 mm intervals. The striping of the acrylic jacket on the fiber allowed the hydrogen better access to the silica instead of having to diffuse through the jacket and fiber. The fiber was then wrapped around an aluminum support slug. The aluminum also occupied space in the hydrogen loading chamber (O/E Land Inc OEHLS-500) thus decreasing the amount of hydrogen put in the chamber during a loading period. Less Hydrogen in the chamber increases the safety of the loading process. After bolting down the chamber pressurizing with Hydrogen to 2000 psi (1.38×10^7 Pascal), the chamber was then gradually heated for at least three days at 100ºC. When loading was completed, the hydrogen was carefully vented out of the chamber, and the fiber was removed. Quickly the fiber was taken off the spool and put into a freezer to slow the hydrogen diffusion from the fiber. The fiber is then either written quickly to lock in the hydrogen, or put into the freezer for future processing. Unfortunately the process was not optimized and writing a grating with hydrogen loaded commercial fiber took longer than two hours.

Fiber with increased sensitivity to ultra-violet radiation permitted quicker turnaround for gratings by allowing us to bypass the hydrogen loading and long write times. Again 450 mm of fiber was used per device, and the acrylic coating is stripped and swabbed with alcohol to make sure there was no contamination on the surface to interfere with incident UV light, and make certain that the fiber was evenly etched. Contamination in either

case will result in unwanted side effects such as inferior resonant peaks and coarse surface texture, both of which contribute to poor devices.

3.3. Etching

For regular Bragg or long period gratings, grating writing occurs with normal 125 μm diameter fibers. However, in our device the cladding is thinned from 125 μm to approximately 30-40 μm. Etching of the silica was accomplished using a standard hydrofluoric (HF) acid bath. Our bath consisted of 26% HF dissolved in water with no buffers. The high concentration of HF allowed for a quick (~2 hour) etch of a 125 μm fiber down to approximately 35 μm. The reaction for the etching process involved using the HF acid to convert the silicon dioxide into silicon hexafluoride.

$$SiO_2 + 6HF \rightarrow H_2 + SiF_6 + 2H_2O$$

The exact diameter of an etched fiber was often determined during the etch process with a micron meter measurement on test fibers that were easily pulled from the bath and rinsed. Because the etching used an HF solution that was not buffered, the etching times slightly increased from batch to batch. This was attributed to the fact that the fluorine was gradually consumed in the etch reaction something the buffered etching overcomes. When etch times for 80 μm of silicon reached a length greater than approximately 3 hours, a new 26% HF solution was blended. To increase throughput and decrease losses due to the very fragile nature of thin cladding silica fibers, a Teflon frame held multiple fibers for the duration of the etch bath. The holder allowed five or more fibers to be

etched in a batch, and it propped up the fibers, so the HF solution could flow completely around it. This insured the uniformity of the final etched fiber and allowed the use of a Teflon stirrer to mix the HF acid during the process and help insure the etching was uniform. After thorough cleaning with a basic solution of sodium hydroxide and water, the fiber is then ready for either an inner conductor sputtering or direct writing of the long period grating.

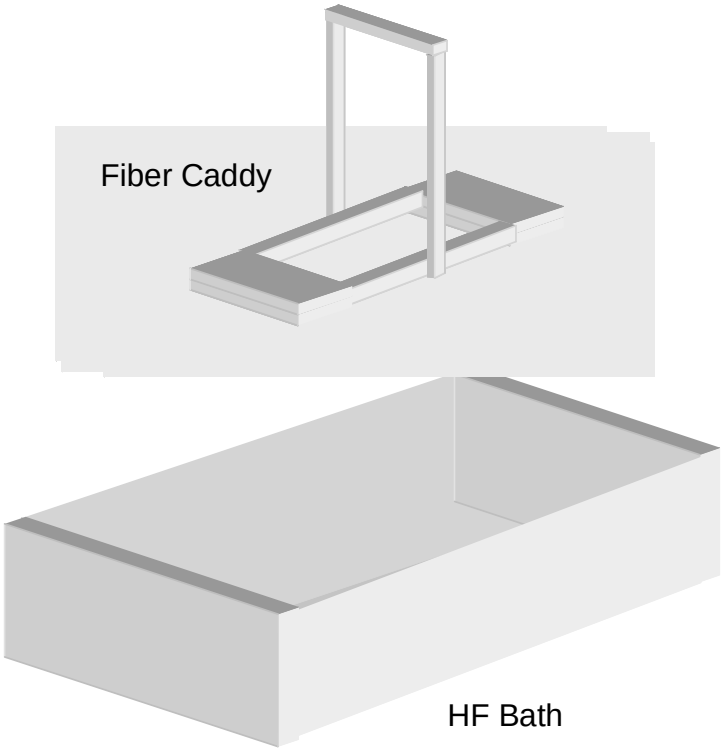

Figure 9. Fiber caddie and Hydrofluoric acid bath.

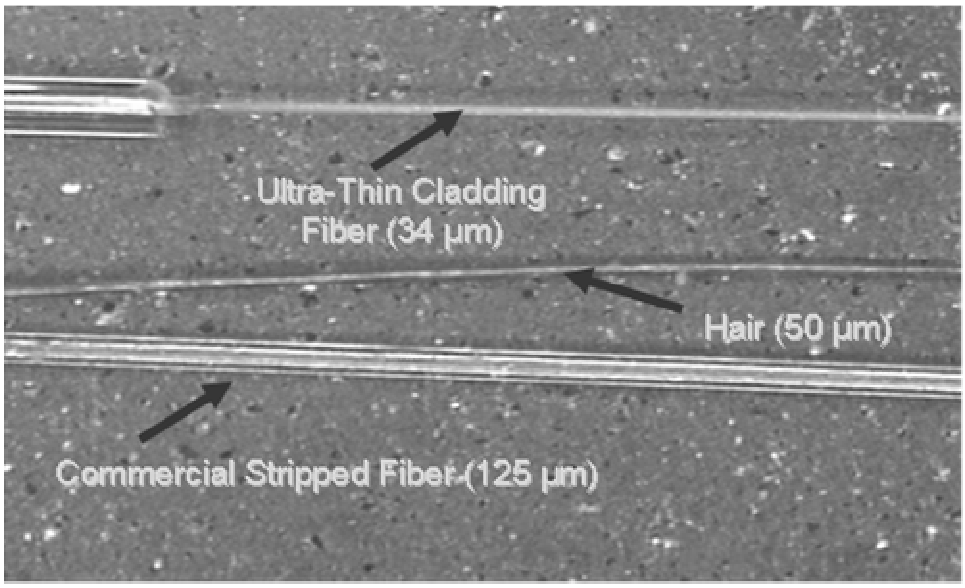

Figure 10. Comparison of ultra-thin cladding fiber with hair and normal fiber.

3.4. Indium Tin Oxide Sputtering

Sputtering of a thin transparent conductive layer on the thin cladding fiber provides the device with an inner conductor. Indium tin oxide is often used for thin, transparent, conductive films, because of its transparency in the visible regions of the spectrum and its ability to be sputtered as a thin coating. It was our goal to sputter a coating that was tens to hundreds of nanometers thick. Etched fibers are first mounted on a substrate plate inside the Anatech Hummer XII vacuum chamber with adhesive tape. The cavity is pumped down to 2×10^{-6} torr, and argon gas is released into the chamber at a pressure of 5 mtorr. Magnetron radio frequency sputtering was then used to excite and ionize the argon atoms. Thirty Watts of power for 15 minutes was used to coat one side of the fiber. The chamber was then pressurized, the samples turned over 180 degrees, and pumped down again to vacuum for sputtering the other side of the fibers. Since the fibers are

cylindrical in shape the sputtering from one direction causes lobes to form on the surface. Effects from these lobes did not seem to affect the conductivity of the thin layer, but in future devices this is one area that must be addressed so as to control possible polarization effects in the final filter design as well as other non-uniform side effects.

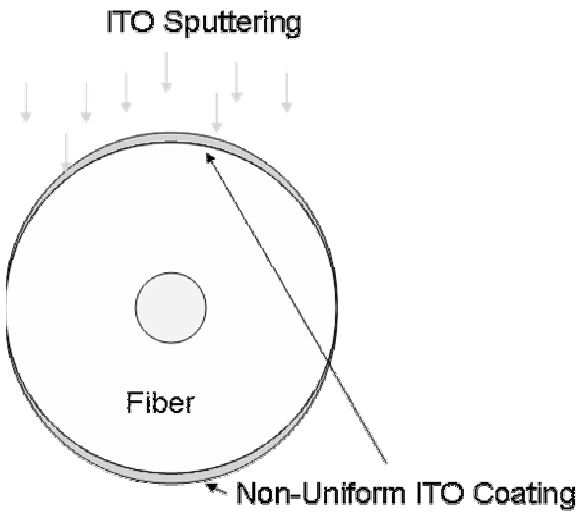

Figure 11. Indium tin oxide sputtering forms a non-uniform inner conductive layer.

3.5. Grating Writing

The next step in the device production involved actually making the index grating structure. For this step, a continuous wave argon ion laser (Coherent Innova Sabre MotoFred Ion Laser System) with a frequency doubling crystal produced the desired ultraviolet wavelengths. Argon ion lasers have a lasing line at 488 nm, and after passing through a Beta-Barium Borate (b-BaB_2O_4 or BBO) crystal the frequency doubled 244 nm UV light emerges to write defects into the hydrogenated or photosensitive fiber. The

actual grating periods in the devices were not less than 150 μm because of the extreme expense in purchasing an amplitude mask with such short periods.

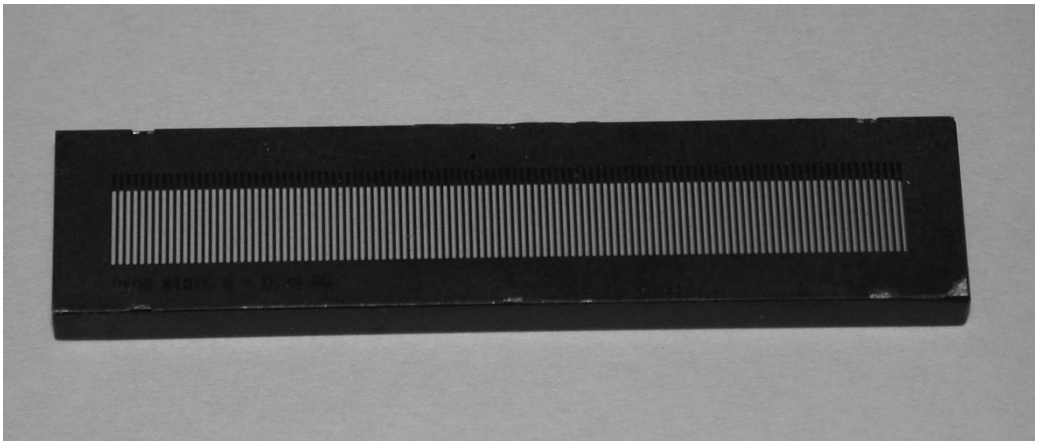

Figure 12. Amplitude mask with period 500 μm.

A fiber was mounted on a nano-positioning stage (Aeroteck), and adjusted to be level and plum with the movement of the stage to insure that the gratings being written were perpendicular to the fiber's length. The laser beam was kept at a constant position, and the stage with mounted fiber and mask was rastered across the laser beam. An optical spectrum analyzer attached to the fiber allowed real-time monitoring of the fiber while a laser wrote the grating. The movement of the stage was computer controlled, and followed programs written by an operator for the entire process. Mounting the fiber on the bracket system was completed with great care because the fiber was even more fragile than normal due to its reduced diameter.

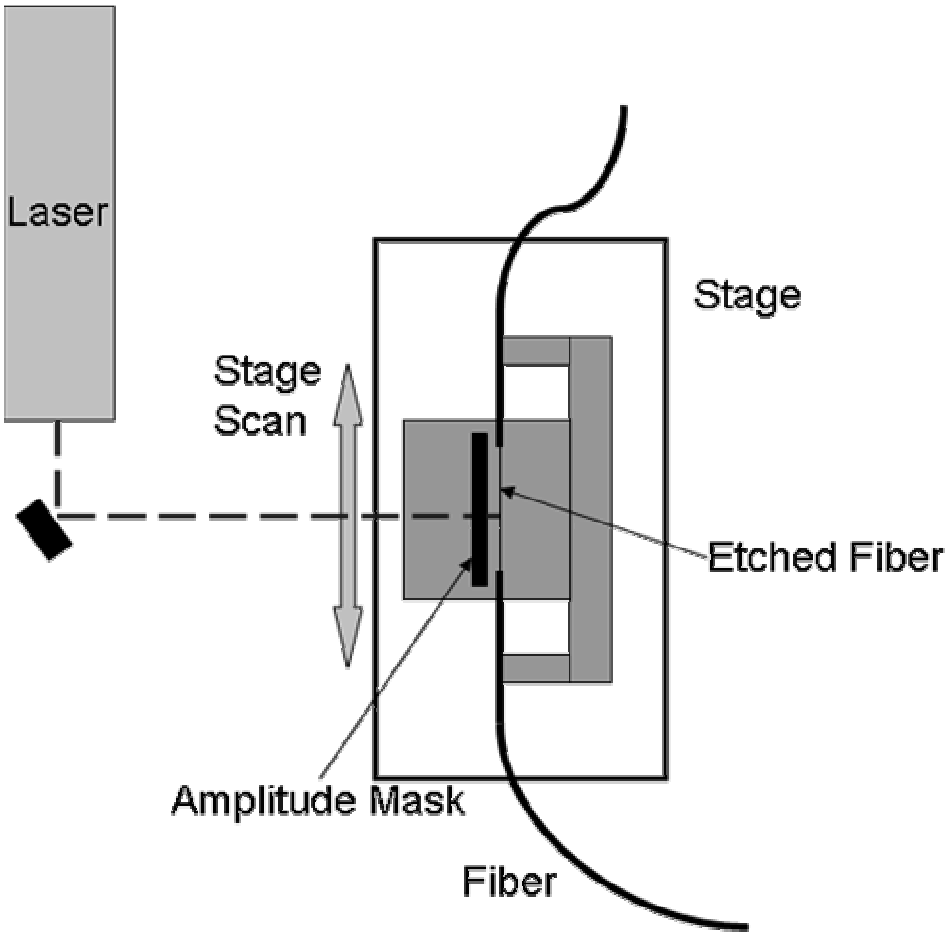

Figure 13. The stage and laser setup used to write gratings into fiber.

The scanning procedure had many variations to produce gratings with different characteristics such as deep nulls or narrow bandwidths. The initial approach involved a smooth scanning back and forth over the fiber through the amplitude mask. For example, one method used a 500 μm period mask and scanned a section of fiber 30 mm long many times until the grating would produce a desired null depth. Often the max null observed from this procedure was 12 dB and not impressive. Later after experimenting with procedures, it was found that if the UV light was left on one spot or area for an extended time (>5 min at 250 mW), the grating produced had a deeper null (20 dB) but had a

slightly larger bandwidth. This was probably due to the amount of energy being absorbed into the fiber for defect creation. When the beam was stationary, more energy was being coupled into the grating while when the laser was rastering across the fiber constantly the time over a specific spot for writing was limited by the beam size.

In one example, a fiber was etched to 34 μm in diameter with no ITO coating. The fiber was then written with 250 mW of UV power and a 350 μm amplitude mask. The scanning procedure left the UV source with a beam size of 2.1 mm stationary on the mask and fiber for five minutes and then moving the spot 1 mm and repeating eight times. The figure below shows the progression of the spots after five minutes.

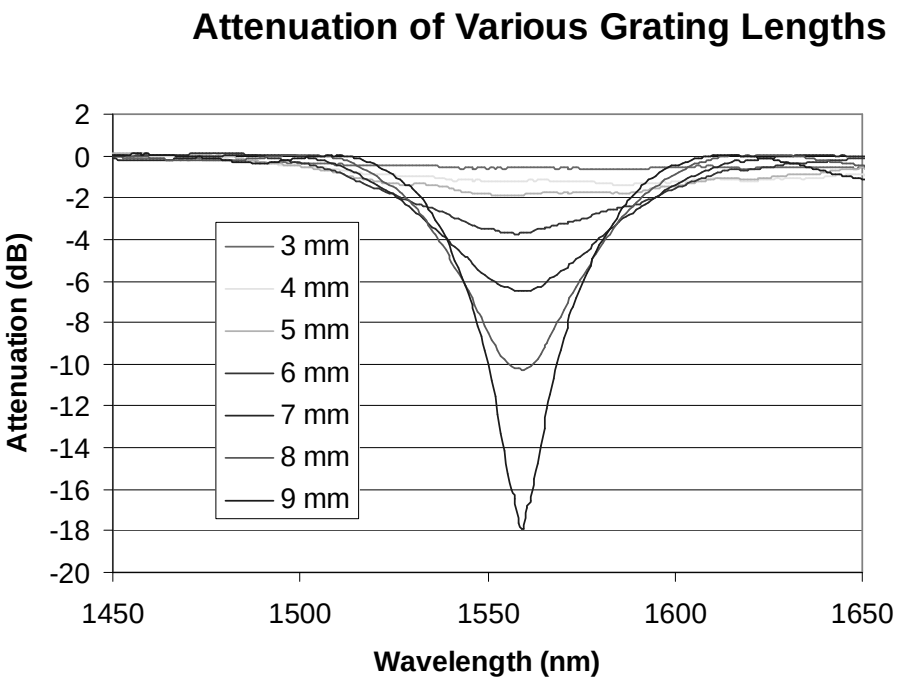

Figure 14. Long period grating's resonant band development during the writing process.

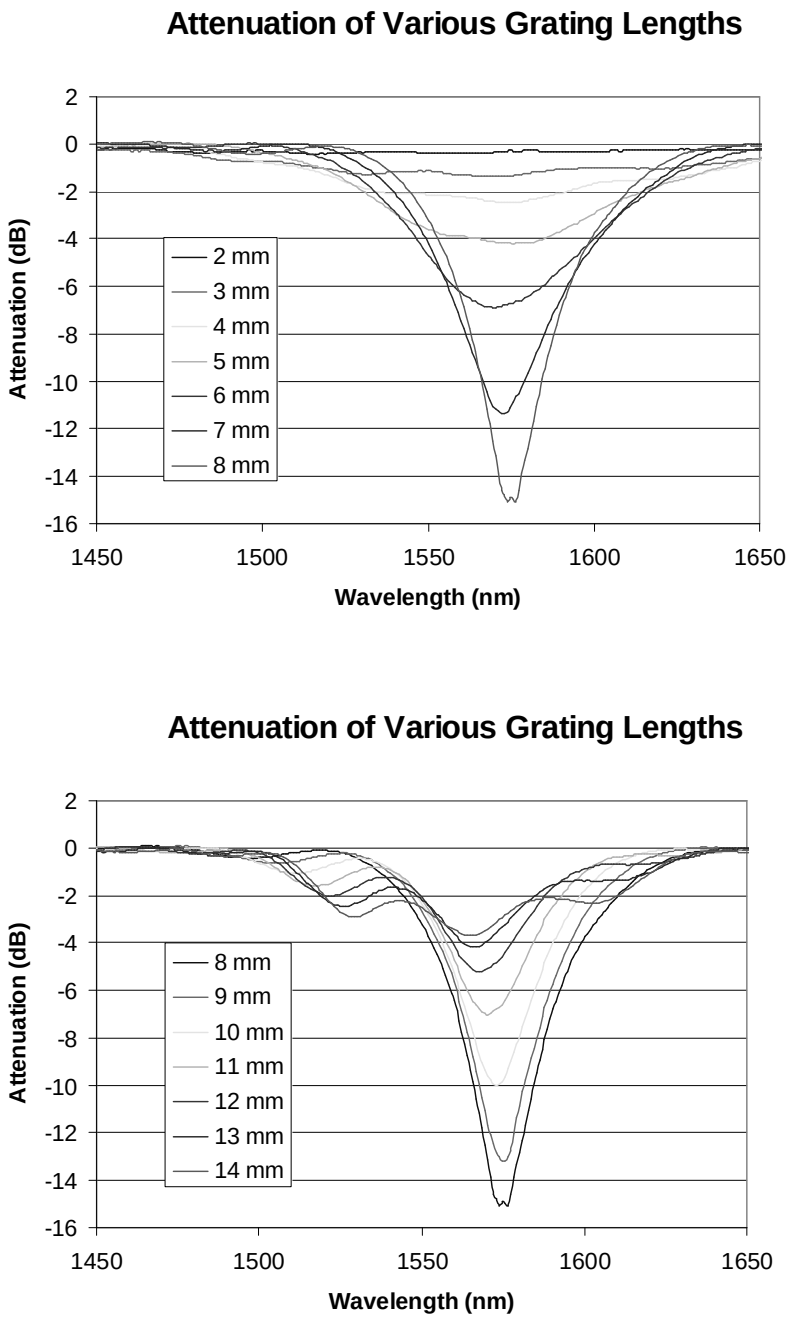

Figure 15. As the number of gratings increase, the coupling of light into the cladding modes varies sinusoidally.

Since the beam emanating from the laser is Gaussian, and the movement of the spot was less than half of the beam diameter, all that this approach does that the scanning mechanism does not was allow more energy from the UV laser to create defects in the fiber before moving on, essentially a very slow scan. The scanning motion which ran at 50 mm/min was too fast and when significantly slowed down also produced 20-25 dB nulls. It should be noted here as well that making the grating longer does not produce a deeper null. An optimum length in the grating produces maximum coupling between the forward propagating core and cladding modes. The coupling varies sinusoidally with grating length, and causes the resonant band created by the coupling to appear and disappear as a grating is elongated.

3.6. Polymer Application

Application of the polymer to the gratings was accomplished by applying the polymer to the surface in several ways. In one example, a ferro-electric polymer that can change density and thus index with an applied electric field, was simply applied over the fiber in a roughly cylindrical manner and cured by hand. This introduces a lot of variables in device performance that cannot be exactly repeatable but was able to show the basic concept at work.

In another case a liquid crystal polymer was applied to a fiber by sandwiching the polymer with the fiber between two ITO coated slides. This structure produced a parallel plate capacitor for switching the liquid crystal and thus index, but the cylindrical nature

of the device has been given up and thus polarization effects start to appear not only based on the device structure, but the liquid crystals themselves.

3.7. Final Packaging

The final steps to device design are sputtering of the outside electrode and encasing the device in a robust housing. Aluminum or gold was applied to the polymer surface to allow for a conductive layer onto which the second electrode to the devices cylindrical capacitor. Care had to be taken to allow for an electrode from the inner ITO layer not to be shorted by the application of this metal layer. When sputtering, a protective covering was placed on the area to be used for ITO contact. When complete and tested again to make sure the device is still operating properly, the device is ready for filter performance testing and final packaging.

Packaging a device entails putting it inside an aluminum tube with holes for the fiber and two electrodes for voltage control over the second cladding layer. We have done only preliminary packaging experiments to insure that packaging of the device would be possible. All of the devices produced have been used for performance testing and have not yet progressed to this stage. Experiments on other devices which rely on thermal tuning were used instead to test the packaging size and feasibility. One of the main focuses of the testing was getting the lead wires for the heating mechanism in and out of the aluminum casing with out damaging the devise itself.

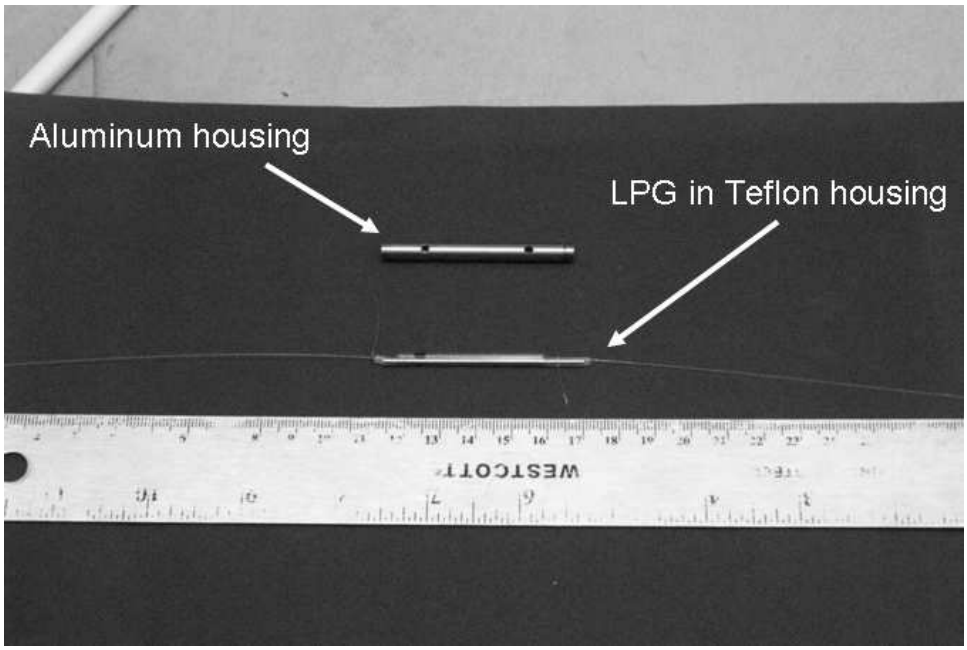

Figure 16. Final aluminum housing and device placed in protective Teflon jacket.

Chapter 4

Results

4.1. Introduction

Over the course of the research improvements in both long period grating fabrication and overall filter design were made. At first the emphasis was on writing gratings to photosensitive single mode fiber, and then later, incorporation of the thin cladding design to produce single resonant band gratings was implemented. Later, refining the process to produce gratings with better filter characteristics and then incorporating them into an overall device with ITO and polymer layers was completed. The results from gradual filter improvement starting from the early LPGs and then the latest filter performance is presented.

4.2. Early Experiments

Creating an LPG from a stripped photosensitive fiber was one of the first experiments conducted. Using the grating writing setup and a single mode fiber, many gratings were fabricated with grating periods ranging from 150 – 500 μm. An example of many of the gratings that were produced was a grating that has a 500 μm period length and a total grating length of 35 mm or approximately 70 periods.

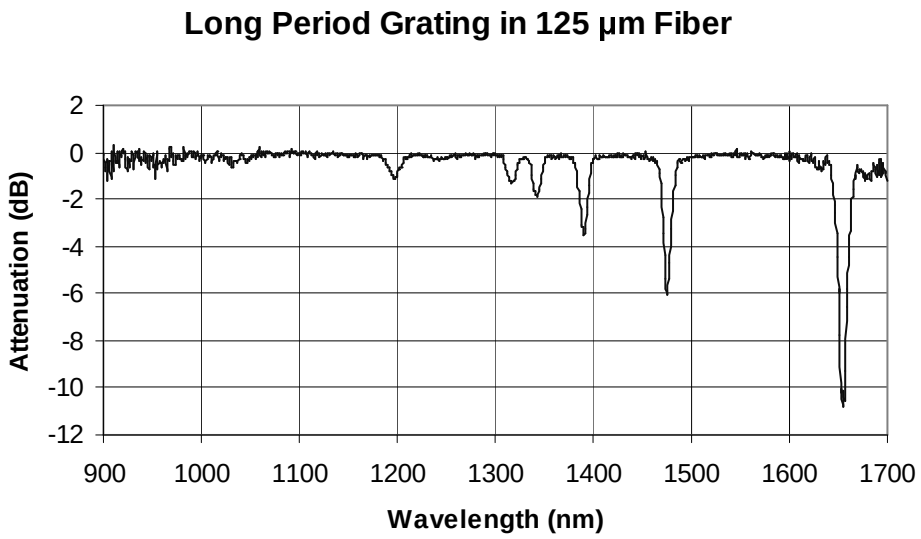

Figure 17. Long period grating in a 125 μm fiber with period of 500 μm.

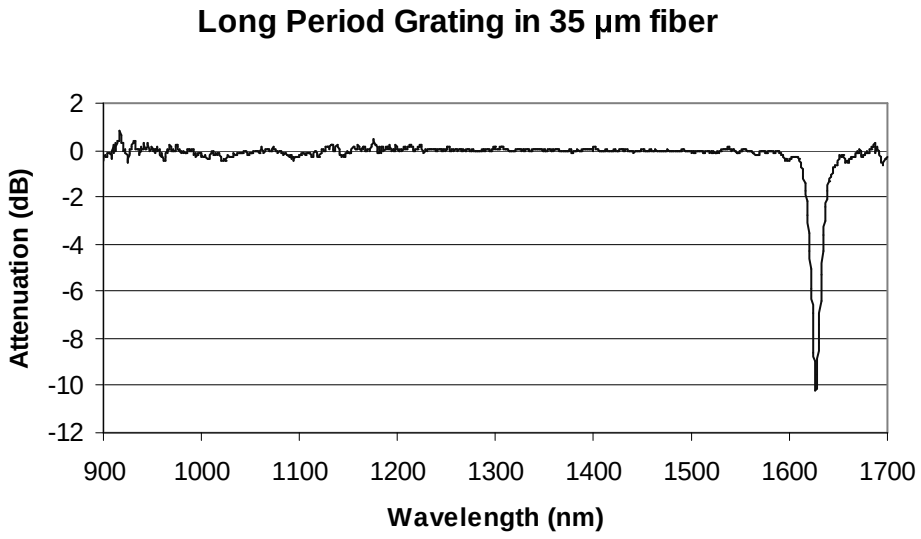

Figure 18. Long period grating in a 35 μm fiber.

The transition from the multiple modes being coupled in the 125 μm case and the single mode coupling in the 35 μm case can easily be seen. A lot of time was dedicated making the writing process efficient and fruitful. Fibers with diameters on the order of 35 μm are very fragile and learning to handle such delicate objects was time consuming.

4.3. Tuning with Second Cladding Layer

The next stage of the research involved verifying previous work on changing the second cladding layer's refractive index and thus changing the effective refractive index of the cladding. Tuning the resonant band with different third layer materials was accomplished two different ways. By using ambient air as one medium and water as a second with indices of 1.0 and 1.33 respectively and then dipping the LPG in water, a shift could be measured and seen easily. The recorded response of the filter between air and water could be visibly seen although very small (4 nm). It was enough of a confirmation to move on to materials that exhibit refractive indexes that were much closer to the index of the second cladding layer. With indices so close, a small change in index in the third layer could produce a much larger change in resonant wavelength than that seen in the water/air experiment.

Tuning with index matching oils allowed a tailoring of the second cladding layer index and thus a much larger change in coupled wavelength. As the oil's index approached the index of the first cladding layer, the resonant wavelength was again pushed farther into the shorter wavelengths. A photosensitive fiber with a diameter of 42 μm had a 500 μm grating written to it. The fiber was then dipped into progressively higher index oils with a

thorough cleaning of the fiber with alcohol between each stage. The wavelength the resulting three layer device tuned a larger distance as expected (~25 nm). The large tuning range confirms that if the third layer of the tuning device can be manipulated, the single resonant band created by the LPG and the thin cladding can be used as a filter device.

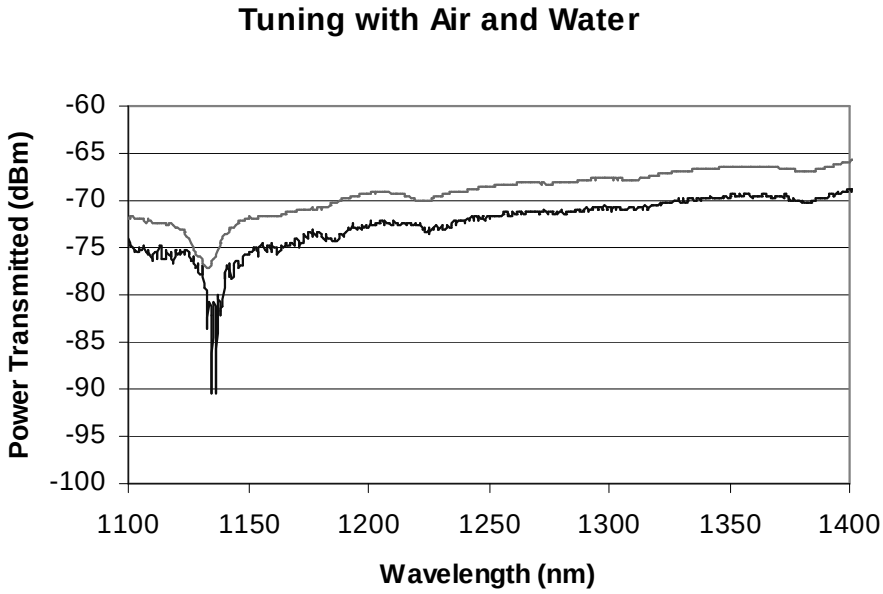

Figure 19. Tuning a long period grating by 4 nm with water and air.

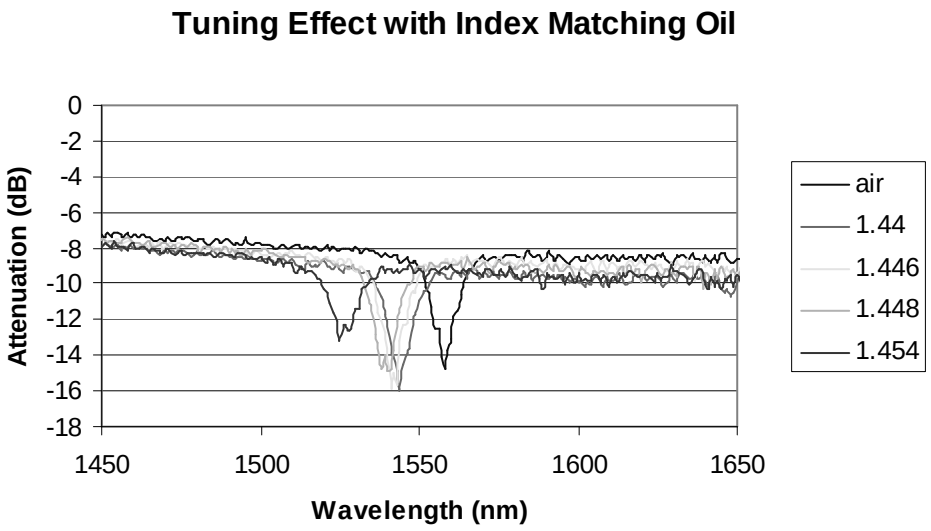

Figure 20. Tuning effect using index matching oils.

4.4. Ferro-electric Polymer Device

The first of the polymers to be tested was a ferro-electric polymer. After application of the ITO and the writing of a 500 μm grating, the polymer was applied to the surface of the device. Then after approximately 30 μm of polymer had been cured on the surface of the device, a gold outer conductor was sputtered on the surface of the polymer. The device was then tested with a high voltage source to change the index of the polymer. Again the change in filtered wavelength was only 6 nm, but this was a first successful test and further testing and tuning of the polymer may produce larger tuning ranges. In the future this polymer has to be tailored so that it matches the index of the first cladding layer much like the index matching oil experiment. Once the polymer is engineered to the correct index a wide tuning range can be produced.

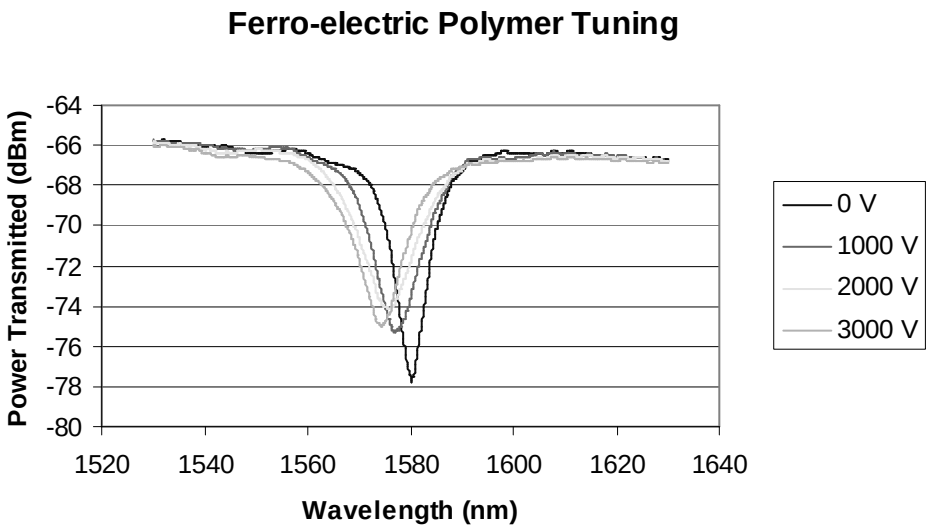

Figure 21. Device tuning of 6 nm with ferro-electric polymer.

4.5. Liquid Crystal Device

Liquid crystals were also utilized as a tuning mechanism. Using a UV curable polymer embedded with liquid crystals in between two conductive plates of ITO coated glass provided enough change in index when a voltage was applied to record a tuning effect. The liquid crystals were mixed into the UV curable polymer and sandwiched with the fiber grating in between the two ITO glass plates. Using UV light, much like that in lithography, the polymer was hardened with the liquid crystals inside. Electrodes were then attached and used to align the liquid crystals. Again this simple experiment did not have a wide tuning range, but it was able to demonstrate the tuning of the filter using a polymer that was controlled by a voltage.

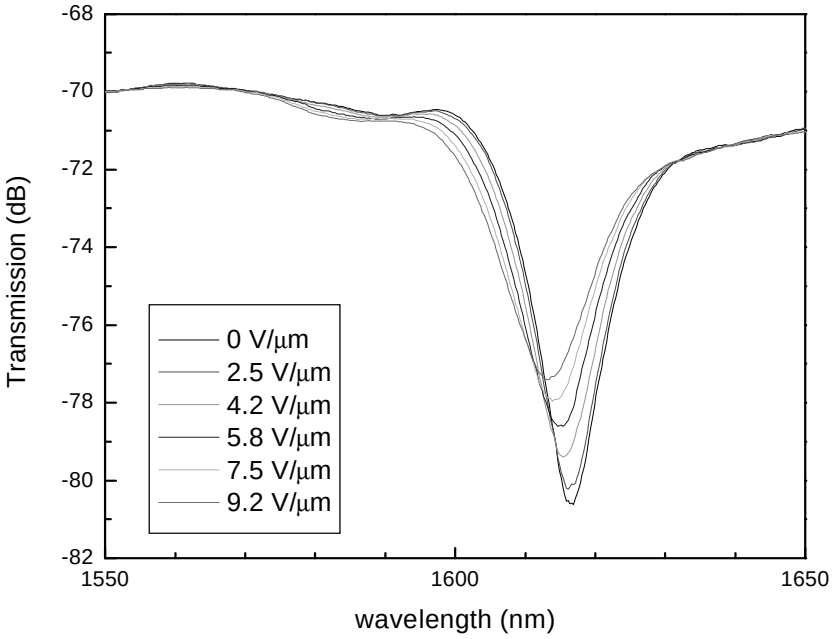

Figure 22. Tuning with liquid crystal polymer.

Chapter 5

Conclusion

Using a long period grating as the basis of the device does prove to be an excellent way to build a flexible optical filter. By enhancing the long period grating coupling to allow only a single resonant band to pass from the core to the cladding, the filter's tuning range can be enlarged. Then by using an electro-optic polymer as a third layer or second cladding, the device can be tuned quickly because of the response time of the polymer to an electric field. The polymer also permits the device to be completely solid state and thus useful in many applications were mechanical or thermal filters would not hold up to extreme environmental conditions.

Coupled mode theory is essential to understanding the mechanics behind the operation of the long period gratings. By utilizing this theory, a model can be developed to predict the behavior from a constructed grating, and it allows us the ability to understand how to tweak the manufacturing process to produce different characteristic gratings with deep nulls or small bandwidths, for example.

When producing a grating from common commercial fiber, it is necessary to load the fiber with hydrogen. This allows the defects in the fiber to form when the hydrogen combines with the fiber chemistry during UV illumination. Another important process is the sputtering of material forming very thin films on the surface of the device. An

understanding of sputtering and thin film deposition science is needed if quality films are needed.

Procedurally, the device manufacturing is a lengthy process with many steps and caveats. Chapter three delves into as many of the facets of producing the ultra-fast, all fiber filter and if it is possible. Development of the photosensitive fiber or commercial single mode fiber all the way to final testing is covered and examined. No doubt, as future work on this device is done these processes and procedures will likely change. This chapter also illustrates some of the flexibility in the process, such as the order in which the fiber is etched and written. It was found that these processes could be reversed and that certain advantages arise from the order.

The results of the testing at first just confirmed what was being done in the area with simple air and water tests. Then experiments using index oils for the third layer of the device are reported. As the device becomes more mature, branches are developing in the polymers that are used in the third layer. Control of this third layer index by means of electro-optic effect, ferro-electric effect, or even the use of liquid crystals has demonstrated the unique properties of each. Utilizing these properties would allow a filter to be built for specific applications that demand high switching speed or environmental robustness, and then be able to tailor the polymer used to that application. The device already has low insertion loss due to its all fiber design, but the goals of 0.1 nm 3dB bandwidth and 50 nm tuning were not realized at this juncture. Further research into the polymer index matching and LPG device structures will yield better results.

References

[1] J. M. Lopez-Higuera, Handbook of Optical Fiber Sensing Technology, John Wiley and Sons Ltd., Chichester, England, 1990

[2] D. K. Mynbaev, Fiber-optic Communication Technology, 2001, Prentice Hall, Inc., Upper Saddle River, New Jersey.

[3] A. M. Vengsarkar, P. J. Lemaire, J. B. Judkins, B. Bhatia, T. Erdogan and J. E. Sipe, "Long period fiber gratings as band-rejection filters," J. Lightwave Technol., vol. 14, pp. 58-64, 1996

[4] V. Bhatia, Ph.D. dissertation, Virginia Polytechnical Institute and State University, 1996.

[5] B. Lee, Y. Liu, S. Lee, S. Choi, and J. Jang, "Displacements of the resonant peaks of a long-period fiber grating induced by a change of ambient refractive index," Opt. Lett., vol. 22, pp. 1769-1771, 1997.

[6] H. J. Patrick, A. D. Kersey, and F. Bucholtz, "Analysis of the response of long period fiber gratings to external index of refraction," J. Lightwave Technol., vol. 16, pp. 1601-1612, 1998.

[7] A. Abramov, A. Hale, R. Windeler, and T. Strasser, "Widely tunable long-period fiber gratings," Elect. Lett., vol. 35, pp. 81-82, 1999.

[8] S. Yin, K. Reichard et al "Wavelength tuning range enhanced single resonant band fiber filter using a long period grating (LPG) with ultra thin cladding layer," OFC 2000, at Baltimore, MA.

[9] S. Yin, K. Reichard et al, "Single resonant band, tunable optical fiber wavelength filter based on long period fiber grating," US Patent 6,563,985

[10] S. Yin, K. Chung, and X. Zhu, "Highly sensitive long period grating based tunable filter using a unique double-cladding layer structure," Optics Communications, v 188, pp. 301-305 (2001).

[11] S. Yin, K. Chung, and Xin Zhu, "A novel all-optic tunable long-period grating using a unique double-cladding layer," Optics Communications, v. 196, pp. 181-186 (2001).

[12] K. Chung and S. Yin, "Analysis of random grating period and amplitude errors in ultra-thin long-period grating," Microwave and Optical Technology Letters, Vol. 12, pp. 178-181 (2001).

[13] Kun-Wook Chung and Shizhuo Yin, "Analysis of a widely tunable long-period grating by use of an ultra thin cladding layer and higher-order cladding mode coupling," Optics Letters, Vol. 29, pp.812-814 (2004).

[14] Turan Erdogan, "Cladding-mode resonances in short- and long- period fiber grating filters," J. Opt. Soc. Am. A, 14, pp. 1760-1773, 1997.

[15] C. Tsao, Optical Fiber Waveguide Analysis, Oxford, New York, 1992.

[16] Joo-Nyung Jang, Se Yoon Kim, Sun-Wook Kim, and Min-Sung Kim, "Novel temperature insensitive long-period grating by using the refractive index of the outer cladding," OFC 2000, at Baltimore, MA.

[17] J. D. Plummer, M. D. Deal, P. B. Griffin, Silicon VLSI Technology, Prentice Hall, Inc., Upper Saddle River, New Jersey, 2000

[18] K. Chung, Ph.D. dissertation, Pennsylvania State University, 2000.

[19] T. Gerfin and M. Gratzel, "Optical properties of tin-doped indium oxide determined by spectroscopic ellipsometry", Journal of Applied Physics, 79 (3), Feb 1, 1996, p. 1722-29.

[20] "ITO, Tin-Doped Indium Oxide for Optical Coating," 2000, Retrieved January 15, 2005, from http://www.cerac.com/pubs/proddata/ito.htm